JOURNAL OF BACTERIOLOGY, Oct. 1992, p. 6198–6206
0021-9193/92/196198-09$02.00/0
Copyright © 1992, American Society for Microbiology
Vol. 174, No. 19

A Three-Start Helical Sheath on the Flagellar Filament of *Caulobacter crescentus*

SHLOMO TRACHTENBERG[1]* AND DAVID J. DEROSIER[2]

Department of Membrane and Ultrastructure Research, The Hebrew University-Hadassah Medical School, Jerusalem 91010, Israel,[1] and Rosenstiel Basic Medical Sciences Research Center, Brandeis University, Waltham, Massachusetts 02254-9110[2]

Received 10 February 1992/Accepted 26 July 1992

An unusual feature in preparations of the *Caulobacter crescentus* flagellar filaments is that some filaments are surrounded by a set of three windings that form a sheath. We provide evidence that the sheath is composed of subunits having a molecular mass of 24,000 Da. We suggest that the sheath could be composed of protofilaments of flagellin wound around the filament.

All flagellar filaments studied to date share a common symmetry and scheme of design and can, in many cases, copolymerize (7, 29, 32, 36, 40–44). To date, all flagellins, the building blocks of flagellar filaments, show a remarkable sequence similarity at the N- and C-terminal regions and have a variable internal region (13, 16). The variable part of the flagellin sequence corresponds to a knobby domain found at the outside of the filament (19, 41).

Caulobacter crescentus has three flagellins with masses of 29, 27, and 25 kDa (8, 14, 20; for complete references, see reference 30), making them the smallest flagellins found in all species of bacteria. The 29- and 27-kDa flagellins are located in the hook-proximal 2 μm of the filament, with the 25-kDa flagellin making up the bulk of the filament (6, 49). The *C. crescentus* flagellin subunits in the filament lack the knobby outer domain found in filaments of other bacteria (41). The genes for the flagellins occur in two clusters; the α cluster contains *flgJ*, *flgK*, and *flgL*, which encode the 29-, 25-, and 27-kDa flagellins, respectively (8, 28), and the β cluster contains *flgM*, *flgN*, and *flgO*, which all encode the 25-kDa flagellins (as cited in reference 30).

The absence of the outer domains results in a narrow filament about 120 Å (1 Å = 0.1 nm) in diameter. With the outer knobs absent, the dominant feature is a set of nearly vertical striations corresponding to the 11 thin protofilaments (or subunit strands). At their ends, some filaments fray, suggesting that the protofilaments may be stable in isolation (see Fig. 2 in reference 41). Structures that appear to be single, long protofilaments, or bundles of them, are frequently seen in micrographs of filament preparations.

What we report here is the appearance of an unusual *C. crescentus* filament; it appears to consist of the usual filament but with a thin, fibrous set of helical windings wrapped around it. Such external features on flagellar filaments are usually called sheaths and have been seen in other strains of bacteria. Historically, the term "sheath" has been used loosely. It has been applied to integral, but perturbed, parts (outer domains) of the flagellin monomers, such as in *Pseudomonas rhodos* (24, 25, 34, 35), *Rhizobium lupini* (23), and *Escherichia coli* (21, 22), which were wrongly believed to be external matter (43, 44). It has been applied also to the external coat of flagellar filaments from *Vibrio cholerae* and *V. metschnikovii* (9) and other gram-negative bacteria. This true sheath appears to be a membranous structure continuous with the lipopolysaccharide layer of the cell wall. It is not clear, however, whether it is part of this layer or not (12, 50). The sheath can be separated as an intact cylinder from the filament.

Certain of the periplasmic flagellar filaments, for example, those of the spirochetes, also have a sheath (3, 31). In this case, the gene contributing to the sheath is known to be a periplasmic protein distinct from the flagellin; it has no sequence homology with flagellin, and unlike flagellin, it is exported to the periplasm by the signal peptide pathway.

Lysed material attached to flagellar filaments in an irregular and patchy way, e.g., in *Bacillus brevis* (4) and *B. stearothermophilus* (2), has been sometimes called sheath. For a detailed description of these phenomena, see reference 38.

The function of the flagellar sheath is unclear. In the case of complex filaments, the apparent external winding permits infection by flagellotrophic phages (23) and also provides increased structural rigidity (18, 26, 34, 35, 43–45). In the case of filaments covered with a true sheath, the current hypothesis suggests its involvement in cellular attachment with surfaces and with other cells at the initial stages of infection (15, 27, 33, 37).

MATERIALS AND METHODS

Bacteria and media. *C. crescentus* CB15 was grown in liquid medium containing (per 1,000 ml) 2 g of Bacto Peptone, 1 g of yeast extract, and 0.2 g of $MgSO_4 \cdot 7H_2O$; 10 ml of 50 mM $CaCl_2$ was added to the medium with the inoculum. Bacteria were grown for ~16 h at 30°C in a well-aerated flask.

Filament preparation. Cells were pelleted by low-speed centrifugation (15 min at ~8000 × *g*), and the supernatant was saved. The pellet was resuspended in 100 mM aqueous ammonium acetate (pH 6.8), and the filaments were detached by vortex mixing for 60 s. After centrifugation, the supernatant was combined with that from the first centrifugation, and the filaments were pelleted at high speed (120 min at ~70,000 × *g*) and resuspended in 100 mM ammonium acetate. The last step was repeated twice.

Electron microscopy. Electron microscopy was carried out at the European Molecular Biology Laboratory, Heidelberg, Germany, using a Philips EM 400 microscope equipped with an anticontaminator as described by Homo et al. (11).

* Corresponding author.

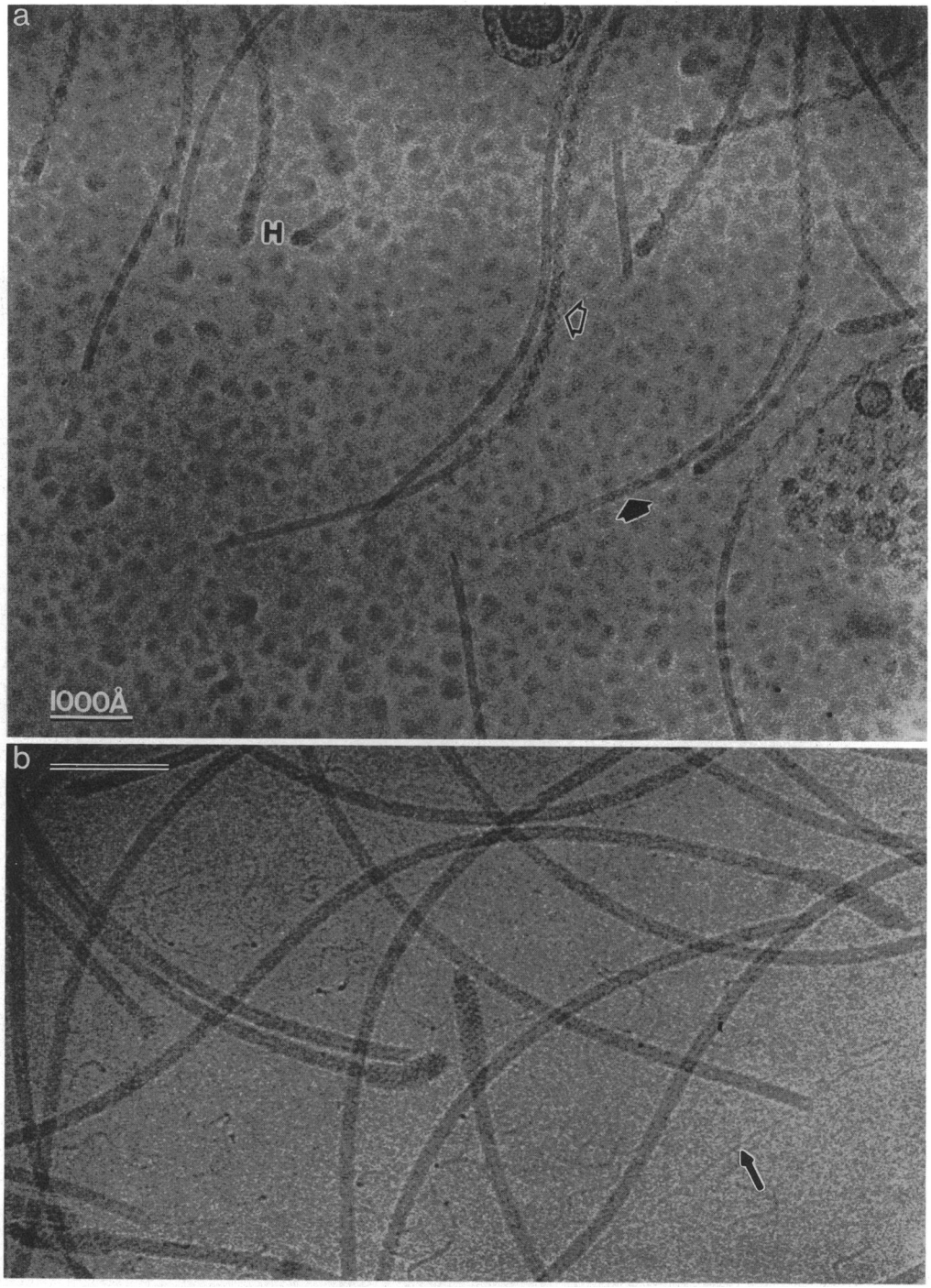

FIG. 1. (a) Frozen-hydrated flagella of *C. crescentus* CB15 suspended over a hole in a carbon film. The filled arrowhead marks an unsheathed filament; the open arrowhead marks a sheathed filament. The sheath consists of a well-ordered, outer three-start winding around the filament. The hook (H) shows clearly the helical grooves not seen in the filaments in panels a and b. (b) Same preparation as in panel a but in which we see thin fibers embedded in the ice (see arrow). Bar = 1,000 Å.

Cryomicroscopy was carried out by using a Gatan model 626 cryo-holder. A thin layer of filament suspension was produced on a holey carbon film and vitrified by being plunged into liquid ethane as described by Trachtenberg and DeRosier (40). Negatively stained specimens were prepared on unsupported carbon films, using 1% uranyl acetate as described by Trachtenberg et al. (44).

STEM. Scanning transmission electron microscopy (STEM) studies were carried out at Brookhaven National Laboratory (48). Specimens were prepared as described by Trachtenberg et al. (43). Linear mass density measurements were carried out according to Hainfeld et al. (10), using tobacco mosaic virus as a mass standard.

Digital image processing. Negatives were digitized on an

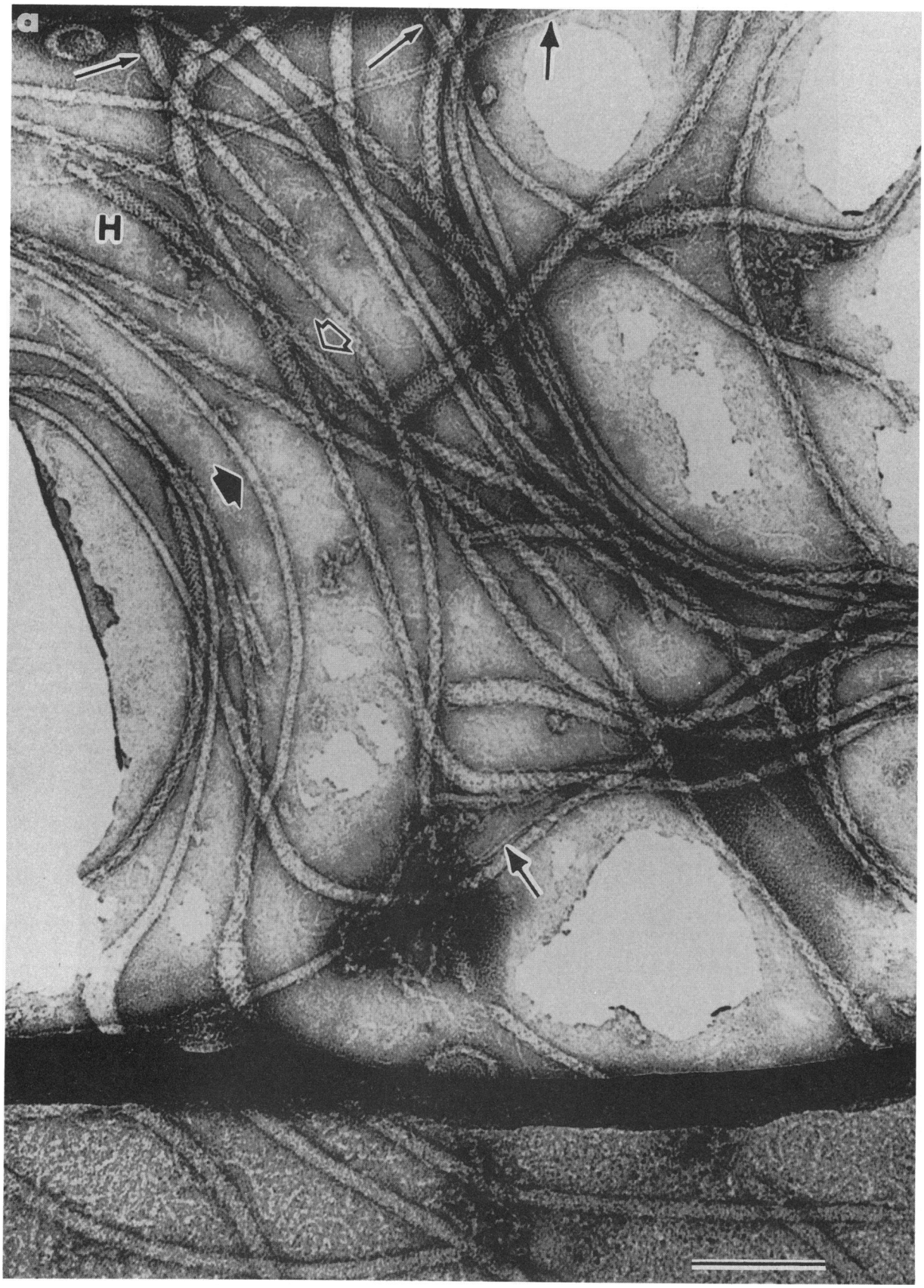

FIG. 2

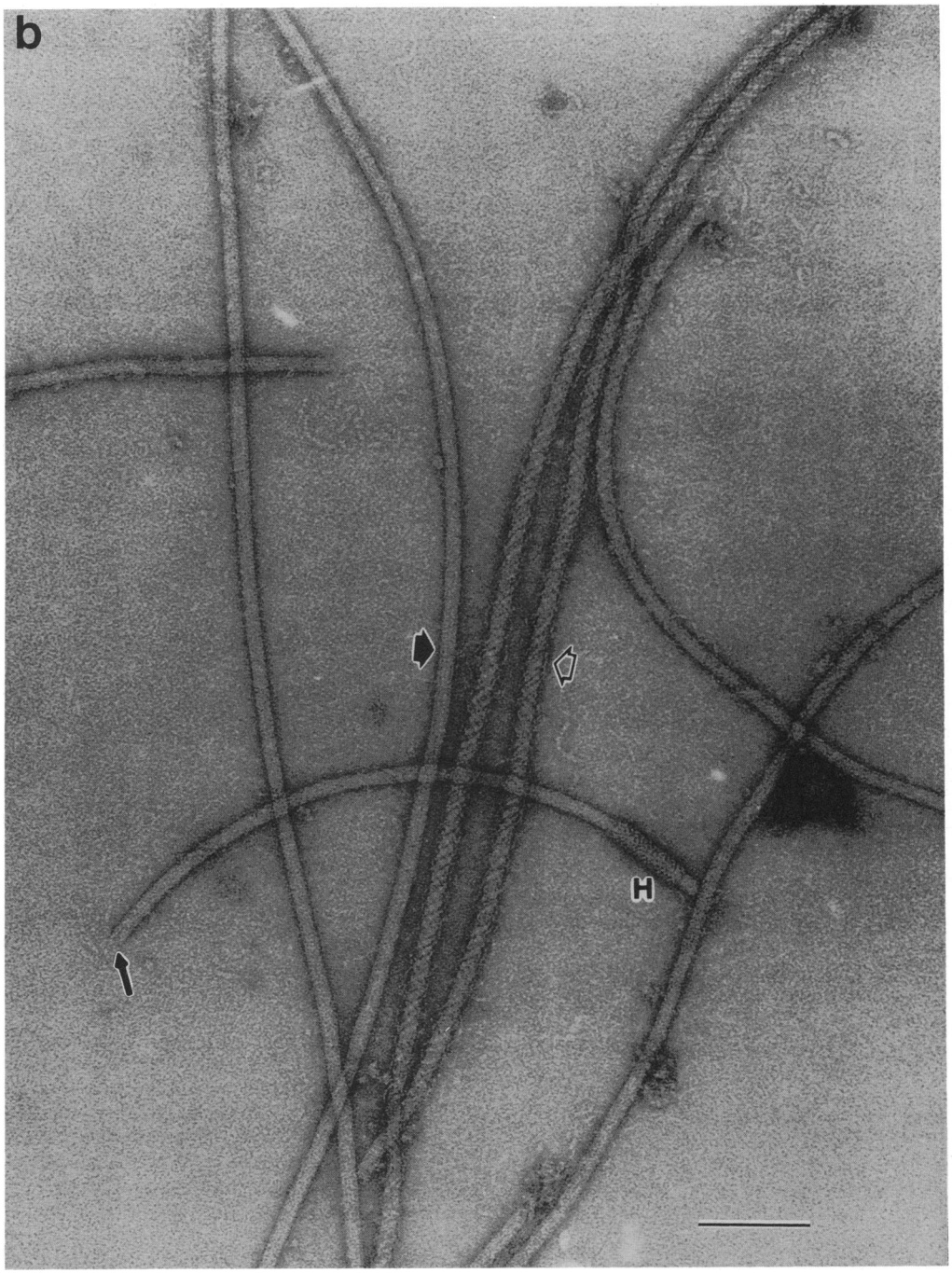

FIG. 2. (a) Negatively stained flagellar filaments. The filaments are embedded in a thin film of uranyl acetate which is suspended over a hole in the carbon film. Unsheathed filaments are indicated by a filled arrowhead, and sheathed ones are indicated by an open arrowhead. Flattened sections of the filaments reveal clearly the protofilaments (thin arrows). Thick arrows mark thin, free, long fibers which we think may be protofilaments. The hooks (H) show clearly the coarse five-start helical grooves. (b) Unsheathed (filled arrowhead) and sheathed (open arrowhead) flagellar filaments supported by a carbon film and negatively stained with uranyl acetate. The protofilaments within the filaments are seen clearly as thin lines almost parallel to the filaments' axes. The sheath around the filaments in the center is clearly visible but not as well ordered as the one in the vitrified specimen. A frayed end is marked with a thin arrow. Bar = 1,000 Å.

Optronics Photoscan P-1000 densitometer at a sampling interval of 25 μm, corresponding to 4.5 Å on the specimen. Diffraction patterns were calculated from the digitized data as described by DeRosier and Moore (5).

RESULTS

The appearance of the sheath. Sheathed filaments are found in most filament preparations. They tend to occur in

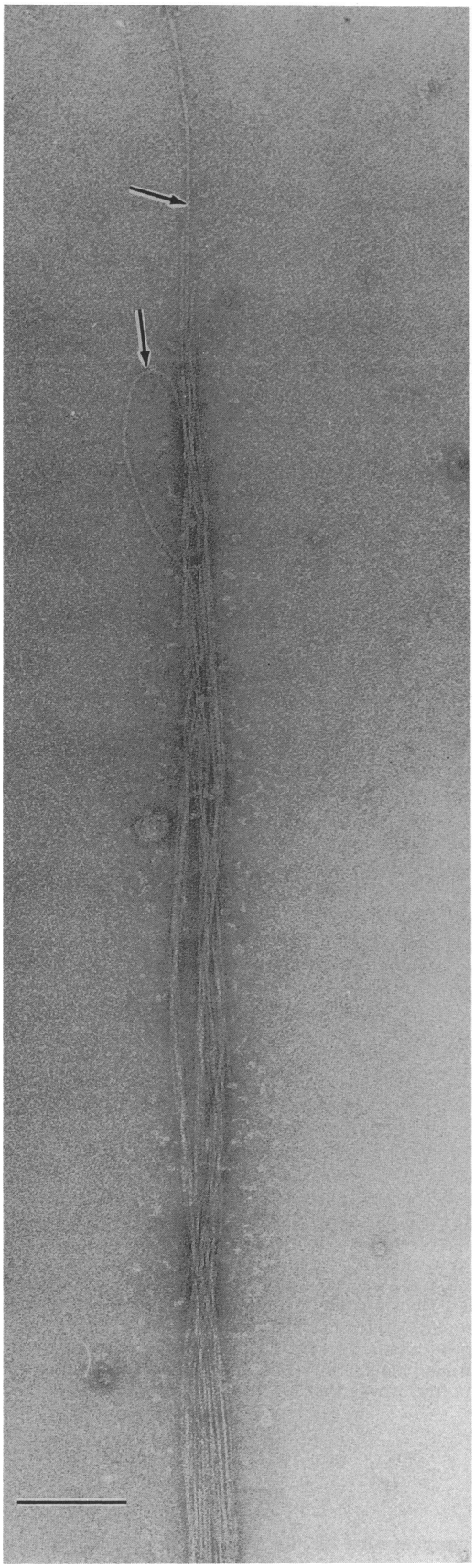

FIG. 3. Bundle of about 12 fibers. Some fine substructure is visible in the individual fibers at the end (arrows). The diameter and general appearance of these fibers are similar to those seen in Fig. 2. Bar = 1,000 Å.

patches surrounded by unsheathed filaments. The proportion of sheathed filaments is nearly impossible to determine quantitatively because of the variability in the preparations, but we guess that they represent less than 10%. The difference between sheathed and unsheathed filaments is clear in Fig. 1. In Fig. 1a, the filament marked by a filled arrow is quite smooth, whereas that marked by the open arrow appears rough. Often, what appear to be pieces of the sheath are seen in the background (Fig. 1b). The sheath is visible both in negative stain (Fig. 2) and in ice (Fig. 1). In stain, the drying deforms and stretches the filament and also appears to unravel the sheath into pieces similar to those in Fig. 1b. The outer windings that have frayed from the sheath are similar in size to the protofilaments of subunits sometimes seen at the ends of filaments (cf. Fig. 2 in reference 41). In rare cases, we see bundles of what appear to be protofilaments (Fig. 3). Whether these arise from the fraying or by the aggregation of material from the medium is unclear.

Relationship of the sheath to the lattice of the filament. The symmetry of the sheathed filaments can be deduced from the diffraction patterns of the images (Fig. 4). The data presented here are from vitrified specimens in which the external sheath seems best preserved. A normal filament, a hook, and a sheathed filament are shown in the left-hand column of Fig. 4; their computed diffraction patterns are shown in the middle column; the corresponding meridionally projected diffraction patterns are shown in the right-hand column. A strong layer line at $\zeta \sim 1/100$ Å^{-1} is clearly visible in the sheathed filament but not in the diffraction patterns of the hook or unsheathed filament. This additional layer line is halfway between the equator ($n = 0$) and the $n = 6$ layer line at $\zeta \sim 1/50$ Å^{-1}, which is seen only in negative stain (41). This marks it as a layer line of order $n = 3$ (see Fig. 6). Thus, there is one winding for every two six-start rows of flagellin subunits in the filament.

Mass per unit length of the sheathed filament. STEM data from freeze-dried filaments are shown in Fig. 5. Note that a small subpopulation of 20 filaments has a linear mass density which is about 1.5 times that of the main population's average. We know that the lower mass density peak corresponds to the more numerous unsheathed filaments (41) and conclude that the smaller but denser peak corresponds to the mass density of the rarer sheathed filament.

FIG. 4. Digital images (left) of a vitrified normal filament (A), a hook (B), and a sheathed filament (C), their computed diffraction patterns (center), and the projection of the diffraction onto the meridian (right). A prominent layer line at about 1/102 Å^{-1} in the diffraction pattern of the sheathed filament corresponds to a layer plane having threefold rotational symmetry, i.e., a J_3 Bessel order (17). This layer line is not present in the diffraction pattern of the hook (note the strong J_6 at 1/53 Å^{-1}) or in that of the filament. The filaments of *C. crescentus*, especially those embedded in ice, diffract very weakly. Compare the vitrified filament's diffraction patterns with the negatively stained ones in studies by Wagenknecht et al. (46, 47) and Trachtenberg and DeRosier (41). Thus, for some of the data needed for this study, we used the layer line spacings obtained previously from filaments embedded in uranyl acetate (41).

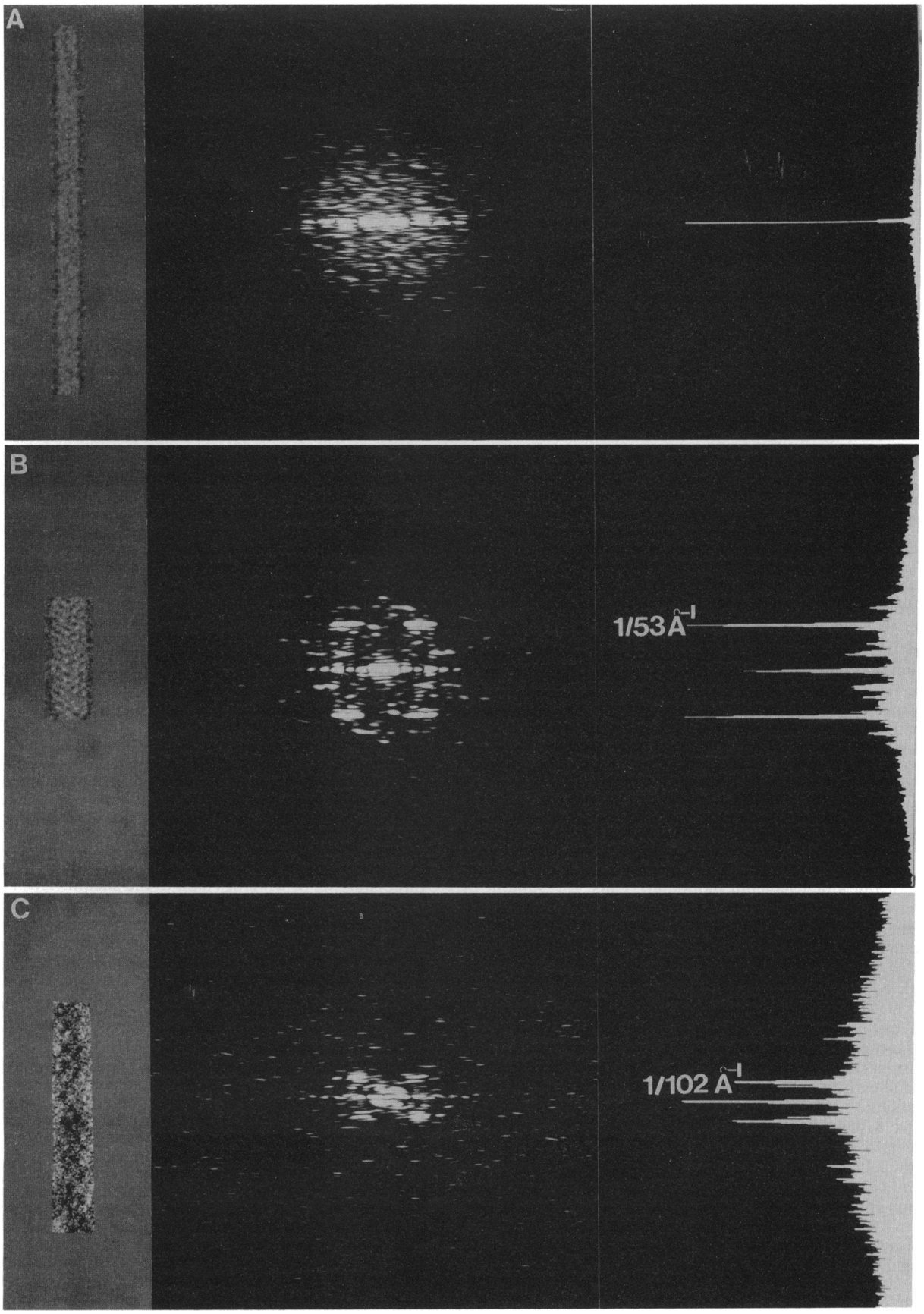

FIG. 4

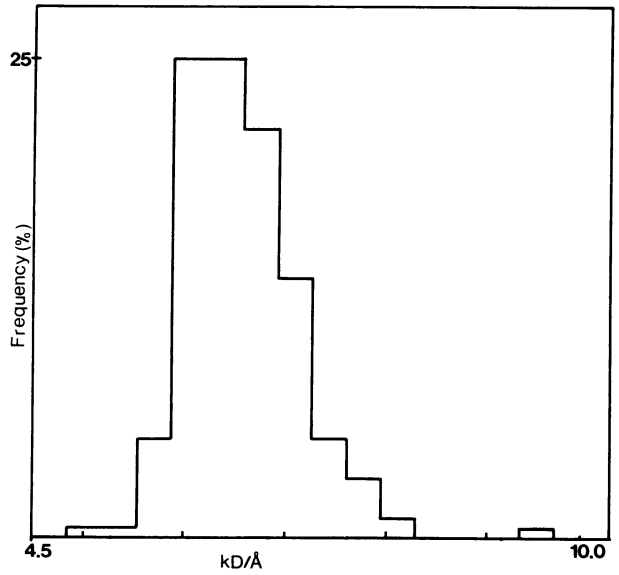

FIG. 5. Histogram showing the distribution of linear mass density measurements of *C. crescentus* flagellar filaments. A small discrete peak (obtained from 20 filaments) of a higher mass corresponds to the sheathed filaments.

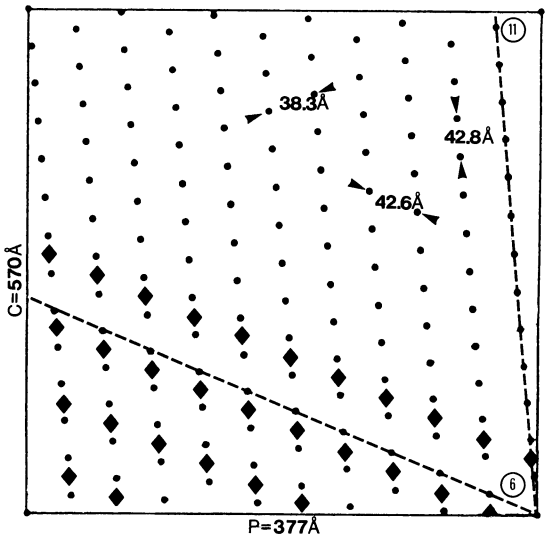

FIG. 6. Unrolled helical net corresponding to the filament (circles) and sheath (diamonds) showing the reduction in the filament's symmetry due to the sheath's presence. The figure is a helical net derived from a diffraction pattern of negatively stained filaments. One helical repeat (C = 570 Å) is shown. The perimeter (P) of the net corresponds to a circumference of 377 Å, the outside circumference of the filament. The subunit spacing along the 11-start lattice lines at this circumference is 42.75 Å, and that along the 6-start lattice lines is essentially the same, 42.59 Å. In contrast, the subunit spacing along the five-start helical line is significantly smaller, 38.34 Å. Thus, a sheath composed of protofilaments could make specific interactions if wrapped about the filament along the six-start but not along the five-start lattice direction. The former situation is shown by the three rows of diamonds. Note there is one sheath subunit (diamond) for every two filament subunits (circles).

DISCUSSION

From the results, we will argue that the sheath is made up of a component having a molecular mass of about 24 kDa. To begin with, the sheath is not a domain of the flagellin monomer as is the case in *R. lupini*. If it were, then the mass of the subunit in the sheathed filament should be 24 kDa (the mass of the flagellin monomer), while that of the unsheathed filament should be significantly less. We determined the molecular mass of the subunits from the linear mass densities. The unsheathed filament has a linear mass density (M_{lf}) of 6.24 (standard deviation = 0.49) kDa · Å^{-1}. The axial rise per subunit (δ_f) is 3.82 Å (41). From these data, we calculated a molecular mass (M_f) for the filament subunit: $M_f = M_{lf} \cdot \delta_f = 6.24 \cdot 3.82 = 24$ kDa. This is the same value that we obtained previously (41), and it equals the molecular mass of the intact flagellin monomer. Thus, the subunit of the unsheathed filament is the whole flagellin monomer, not a fragment remaining after the sheath is cleaved off. We find a second, denser population of filaments which we suggest must be the sheathed filaments. (Fine features such as the sheath cannot be seen in freeze-dried preparations used for mass measurements.) The denser filaments have a higher linear mass density (M_{ls}) than do the unsheathed filaments, i.e., 9.34 kDa · Å^{-1}. We can use the difference in linear mass density of the denser and lighter filaments and the symmetry of the sheath to estimate the mass of the sheath subunit. If we assume, from the reduced symmetry of the sheath relative to the filament, that there is one sheath subunit for every two flagellin monomers (Fig. 6), then the rise per sheath subunit (δ_s) is exactly twice that for the flagellin subunit (δ_f) (i.e., 3.82 · 2 = 7.64 Å). The mass of the sheath subunit (M_s) is, then: $M_s = (M_{ls} - M_{lf}) \cdot \delta_s = (9.34 - 6.24) \cdot 7.64 = 24$ kDa.

The experimental error of this measurement is probably the same as that of the unsheathed filament, about 2 kDa. However, systematic errors, such as partial loss of the labile sheath, could make this estimate of error too low. A related observation, strengthening this point, occurs in studies of Fab-decorated *Salmonella typhimurium* flagellar filaments (39). The mass of Fab fragments (~58 kDa) is very close to that of *S. typhimurium* flagellin (~52 kDa). The linear mass density of a filament decorated to saturation is ~1.5 times that of an undecorated filament, suggesting that the binding ratio Fab/flagellin is 1:2. The Fab units generate an external three-start set of windings akin to the sheath. This is evident in the strong $n = 3$ layer line at 1/100 Å^{-1} in the diffraction patterns taken from electron micrographs. Thus, the binding of an additional protein, in this case an antibody fragment, can produce similar threefold windings and an analogous change in linear mass density.

The sheath we describe here, then, is different from that in *R. lupini*, in which the outer windings arise from the pairwise interactions among outer domains. Instead, in *C. crescentus* filaments, it must result from an additional component that binds to the filament, is easily removed, and hence is not often seen. The puzzle is, where does the material come from? The sheath seems to be distinct from the more substantial sheaths derived from the outer membrane, although we cannot be positive in this case. Since the filament undoubtedly grows at its distal tip, it is hard to see how it could recruit periplasmic subunits. We have no proven answer to the identity of this extra matter, but we do have an interesting, plausible hypothesis: the outer windings are strands of flagellin monomers (i.e., protofilaments). Such a possibility recalls the structures found by Abram and Koffler (1) in the reassembly of flagellin from *Bacillus pumilis* into filaments. Under some conditions, the flagellin subunits

assembled into fine fibers similar, if not identical, to protofilaments. In addition, they found that some of the filaments had a kind of flagellin sheath about them, although not obviously in the form of a set of windings. Thus, there is a precedent for filaments interacting with flagellin protofilaments. There are several pieces of evidence in favor of the view that the *C. crescentus* sheath is made of flagellin. For example, the molecular mass of the putative sheath subunit (24 kDa) is about the same as the masses of flagellins (29, 27, and 25 kDa). We know that flagellin can be exported from the cell and assembles at the distal tip. Perhaps it is possible that the flagellin subunits exported from the cell can assemble into two kinds of protofilaments, one making up the filament and the other making up the windings. Alternatively, the filaments may pick up flagellar protofilaments from the medium, perhaps during filament purification. If the protofilaments indeed form the sheath, then they must interact with the subunits in the filament in a regular way. To do so, the spacing of subunits along the protofilament should be equal to the subunit spacing along the six-start helices (at the outside of the filament). Using a value of 60 Å for the outer radius, we calculated the distances between subunits taken along the protofilament (the 11-start direction) and along the 6-start direction, and, for comparison, the 5-start direction. This is done by measuring distances in an unrolled helical net corresponding to a diameter of 120 Å (Fig. 6). The spacing along the protofilament of 42.75 Å and that along the six-start helix of 42.59 Å are the same, given some uncertainty in the exact filament diameter. The spacing between subunits along the five-start helix is 38.34 Å, much smaller than the other two. Thus, the subunit spacings along the protofilament and six-start direction are the same, within 1%, as required.

All of the available data are consistent with the notion that the sheath is made of protofilaments of one or more of the flagellin. (i) The mass of the sheath subunit is 24 kDa, which is the same as the mass of any one of the flagellins within experimental error; (ii) *Caulobacter* flagellins appear to exist in the form of protofilaments which have dimensions comparable to those of the windings that make up the sheath; and (iii) the spacing of the subunits along the protofilament is exactly that required to interact with the filament along the six-start helical rows. It may be that *C. crescentus* is unique in having such a sheath because it is the narrowest filament. If the filament were wider, the spacing along the six-start would be proportionately longer and the specific interactions between protofilaments and filaments would not be possible. *C. crescentus* is also unusual in having three flagellins. Perhaps one of these makes up the outer winding.

ACKNOWLEDGMENTS

We thank J. S. Wall, J. F. Hainfeld, and P. S. Furcinitti for help with the STEM; A. Driks and T. Wagenknecht for helpful advice and data; and Louise Seidel, Beth Finkelstein, and Phyllis Friedman for typing and editing the manuscript.

This project was supported by grant 87-00039 from the United States-Israel Binational Science Foundation (to S.T.) and grant GM35433 from the National Institutes of Health (to D.J.D.).

REFERENCES

1. **Abram, D., and H. Koffler.** 1964. *In vitro* formation of flagella-like filaments and other structures from flagellin. J. Mol. Biol. **9**:168–185.
2. **Abram, D., A. E. Vatter, and H. Koffler.** 1966. Attachment and structural features of flagella of certain bacilli. J. Bacteriol. **91**:2045–2068.
3. **Charon, N. W., S. F. Goldstein, K. Curci, and R. J. Limberger.** 1991. The bent-end morphology of *Treponema phagedenis* is associated with short, left-handed, periplasmic flagella. J. Bacteriol. **173**:4820–4826.
4. **DeRobertis, E., and C. M. Franchi.** 1951. Electron microscope observation on the fine structure of bacterial flagella. Exp. Cell Res. **2**:295–298.
5. **DeRosier, D. J., and P. B. Moore.** 1970. Reconstruction of three-dimensional images from electron micrographs of structures with helical symmetry. J. Mol. Biol. **52**:355–359.
6. **Driks, A., R. Bryan, L. Shapiro, and D. J. DeRosier.** 1989. Characterization of the proteins of the *Caulobacter crescentus* filament. J. Mol. Biol. **206**:627–636.
7. **Finch, J. T., and A. Klug.** 1972. The helical surface lattice of bacterial flagella, p. 167–177. *In* R. Markham, J. B. Bancroft, D. R. Davies, D. A. Hopwood, and R. W. Horne (ed.), The generation of subcellular structures. North-Holland Publishing Co., Amsterdam.
8. **Gill, P. R., and N. Agabian.** 1983. The nucleotide sequence of the Mr = 28, 500 flagellin gene of *Caulobacter crescentus*. J. Biol. Chem. **258**:7395–7401.
9. **Glauert, A. M., D. Kerridge, and R. W. Horne.** 1963. The fine structure and mode of attachment of the sheathed flagellum of *Vibrio metchnikovii*. J. Cell Biol. **18**:327–336.
10. **Hainfeld, J. F., J. S. Wall, and E. J. Desmond.** 1982. A small computer system for micrograph analysis. Ultramicroscopy **8**:263–270.
11. **Homo, J.-C., F. Booy, P. Labouesse, J. Lepault, and J. Dubochet.** 1984. Improved anticontaminator for cryo-electron microscopy with a Philips EM 400. J. Microsc. **136**:337–340.
12. **Hranitzky, K. W., A. Mulholland, A. D. Larson, E. R. Eubanks, and L. T. Hart.** 1980. Characterization of a flagellar sheath protein in *Vibrio cholerae*. Infect. Immun. **27**:597–603.
13. **Hyman, H. C., and S. Trachtenberg.** 1991. Point mutations that lock *Salmonella typhimurium* flagellar filaments in the straight right-handed and left-handed forms and their relation to filament superhelicity. J. Mol. Biol. **220**:79–88.
14. **Johnson, R. C., D. M. Ferber, and B. Ely.** 1983. Synthesis and assembly of flagellar components by *Caulobacter crescentus* motility mutants. J. Bacteriol. **154**:1137–1144.
15. **Jones, G. W., and R. Freter.** 1976. Adhesive properties of *Vibrio cholerae*: nature of the interaction with isolated rabbit brush border membranes and human erythrocytes. Infect. Immun. **14**:240–245.
16. **Kanto, S., H. Okino, S.-I. Aizawa, and S. Yamaguchi.** 1991. Amino acids responsible for flagellar shape are distributed in terminal regions of flagellin. J. Mol. Biol. **219**:471–480.
17. **Klug, A., F. H. C. Crick, and H. W. Wyckoff.** 1958. Diffraction by helical structures. Acta Crystallogr. **11**:199–213.
18. **Krupski, G., R. Götz, K. Ober, E. Pleier, and R. Schmitt.** 1985. Structure of complex flagellar filaments in *Rhizobium meliloti*. J. Bacteriol. **162**:361–366.
19. **Kuwajima, G.** 1988. Construction of a minimum-size functional flagellin of *Escherichia coli*. J. Bacteriol. **170**:3305–3309.
20. **Lagenaur, C., and N. Agabian.** 1976. Physical characterization of *Caulobacter crescentus* flagella. J. Bacteriol. **128**:435–444.
21. **Lawn, A. M.** 1977. Comparison of the flagellins from different flagellar morphotypes of *Escherichia coli*. J. Gen. Microbiol. **101**:121–130.
22. **Lawn, A. M., I. Ørskov, and F. Ørskov.** 1977. Morphological distinction between H serotypes of *Escherichia coli*. J. Gen. Microbiol. **101**:111–119.
23. **Lotz, W., G. Acker, and R. Schmitt.** 1977. Bacteriophage 7-7-1 adsorbs to the complex flagella of *Rhizobium lupini* H13-3. J. Gen. Virol. **34**:9–17.
24. **Lowy, J., and J. Hanson.** 1964. Structure of bacterial flagella. Nature (London) **202**:538–540.
25. **Lowy, J., and J. Hanson.** 1965. Electron microscope studies of bacterial flagella. J. Mol. Biol. **11**:293–313.
26. **Maruyama, M., G. Lodderstaedt, and R. Schmitt.** 1978. Purification and biochemical properties of complex flagella isolated from *Rhizobium lupini* H13-3. Biochim. Biophys. Acta **535**:110–124.
27. **Meadows, P. S.** 1971. The attachment of bacteria to solid

surfaces. Arch. Mikrobiol. **75**:374–381.
28. **Minnich, S. A., and A. Newton.** 1987. Promoter mapping and cell cycle regulation of flagellin gene transcription in the *Caulobacter crescentus*. Proc. Natl. Acad. Sci. USA **84**:1142–1146.
29. **Namba, K., I. Yamashita, and F. Vondervisztt.** 1989. Structure of the core and central channel of bacterial flagella. Nature (London) **342**:648–654.
30. **Newton, A., and N. Ohta.** 1990. Regulation of the cell cycle and differentiation in bacteria. Annu. Rev. Microbiol. **44**:689–719.
31. **Norris, S. J., N. W. Charon, R. G. Cook, M. D. Fuentes, and R. J. Limberger.** 1988. Antigenic relatedness and N-terminal sequence homology define two classes of periplasmic flagellar proteins of *Treponema pallidum* subsp. *pallidum* and *Treponema phagedenis*. J. Bacteriol. **170**:4072–4082.
32. **O'Brien, E. J., and P. M. Bennett.** 1972. Structure of straight flagella from a mutant *Salmonella*. J. Mol. Biol. **70**:133–152.
33. **Rogers, H. J.** 1979. Adhesion of microorganisms to surfaces: some general considerations of the role of the envelope, p. 20–55. *In* D. C. Ellwood, J. Melling, and P. Rutter (ed.), Adhesion of microorganisms to surfaces. Academic Press, New York.
34. **Schmitt, R., I. Bamberger, G. Acker, and F. Mayer.** 1974. Feinstrukturanalyse der komplexen geisseln von *Rhizobium lupini* H13-3. Arch. Microbiol. **100**:145–162.
35. **Schmitt, R., I. Raska, and F. Mayer.** 1974. Plain and complex flagella of *Pseudomonas rhodos*: analysis of fine structure and composition. J. Bacteriol. **117**:844–857.
36. **Shirakihara, Y., and T. Wakabayashi.** 1979. Three-dimensional image reconstruction of straight flagella from a mutant *Salmonella typhimurium*. J. Mol. Biol. **131**:485–507.
37. **Sjoblad, R. D., and R. N. Doetsch.** 1982. Adsorption of polarly flagellated bacteria to surfaces. Curr. Microbiol. **7**:191–194.
38. **Sjoblad, R. D., C. W. Emala, and R. N. Doetsch.** 1983. Invited review: bacterial flagellar sheaths: structures in search for a function. Cell Motil. **3**:93–103.
39. **Trachtenberg, S.** Unpublished results.
40. **Trachtenberg, S., and D. J. DeRosier.** 1987. Three-dimensional structure of the frozen-hydrated flagellar filament. The left-handed filament of *Salmonella typhimurium*. J. Mol. Biol. **195**:581–601.
41. **Trachtenberg, S., and D. J. DeRosier.** 1988. Three-dimensional reconstruction of the flagellar filament of *Caulobacter crescentus*: a flagellin lacking the outer domain and its amino acid sequence lacking an internal segment. J. Mol. Biol. **202**:787–808.
42. **Trachtenberg, S., and D. J. DeRosier.** 1991. A molecular switch: subunit rotations involved in the right-handed to left-handed transitions of *Salmonella typhimurium* flagellar filaments. J. Mol. Biol. **220**:67–77.
43. **Trachtenberg, S., D. J. DeRosier, S.-I. Aizawa, and R. M. Macnab.** 1986. Pairwise perturbation of flagellin subunits. The structural basis for the differences between plain and complex bacterial flagellar filaments. J. Mol. Biol. **190**:569–576.
44. **Trachtenberg, S., D. J. DeRosier, and R. M. Macnab.** 1987. Three-dimensional structure of the complex flagellar filament of *Rhizobium lupini* and its relation to the structure of the plain filament. J. Mol. Biol. **195**:603–620.
45. **Trachtenberg, S., and I. Hammel.** 1992. The rigidity of bacterial flagellar filaments and its relation to filament polymorphism. J. Struct. Biol. **109**:18–27.
46. **Wagenknecht, T., D. J. DeRosier, S.-I. Aizawa, and R. M. Macnab.** 1982. Flagellar hook structures of *Caulobacter* and *Salmonella* and their relationship to filament structure. J. Mol. Biol. **162**:69–87.
47. **Wagenknecht, T., D. J. DeRosier, L. Shapiro, and A. Weissborn.** 1981. Three-dimensional reconstruction of the flagellar hook from *Caulobacter crescentus*. J. Mol. Biol. **151**:439–465.
48. **Wall, J. S., and J. F. Hainfeld.** 1986. Mass mapping with the scanning transmission electron microscope. Annu. Rev. Biophys. Biophys. Chem. **15**:355–376.
49. **Weissborn, A., H. M. Steinman, and L. Shapiro.** 1982. Characterization of the proteins of the *Caulobacter crescentus* flagellar filament. J. Biol. Chem. **257**:2066–2074.
50. **Yang, G. C. H., G. D. Schrank, and B. A. Freeman.** 1977. Purification of flagellar cores of *Vibrio cholerae*. J. Bacteriol. **129**:1121–1128.